AIAA 96-4505

RESULTS FROM INITIAL OPERATION OF A CONTINUOUS-FLOW, ARC-HEATED HYPERSONIC PROPULSION TEST FACILITY

S.B. Boonjue*, C.M. Roseberry†, and D.R. Wilson'
Mechanical and Aerospace Engineering Department
The University of Texas at Arlington
Arlington, Texas 76019

Abstract

A continuous-flow, arc-heated hypersonic propulsion test facility has been developed at the University of Texas at Arlington. The facility employs a 2.0 MW, vortex-stabilized DC electric arc heater obtained from the Air Force Arnold Engineering Development Center. Descriptions of the arc heater, nozzle, test section, diffuser and vacuum tank; together with the supporting electrical, pneumatic, cooling water, vacuum, instrumentation, and data acquisition/control systems are provided. Calibration data from the initial operation of the facility are presented, and proposed research programs utilizing the new facility for simulation of the off-design performance of hypersonic propulsion nozzles are briefly described.

Introduction

A new continuous-flow, arc-heated hypersonic test facility has been developed at the Aerodynamics Research Center (ARC) at the University of Texas at Arlington. This facility complements the existing test capabilities at the ARC (Fig. 1) by providing a continuous-flow test environment of sufficient duration to investigate a class of hypersonic flow phenomena that are difficult to study in short-duration facilities. These phenomena include, among others, aerodynamic heating, material erosion and ablation, supersonic combustion, hypersonic engine-airframe integration, and stability of hypersonic propulsion systems. The facility was designed to provide the capability of simulating hypersonic flow conditions for aerodynamic testing, or to simulate supersonic combustor exhaust Conditions for hypersonic nozzle testing.

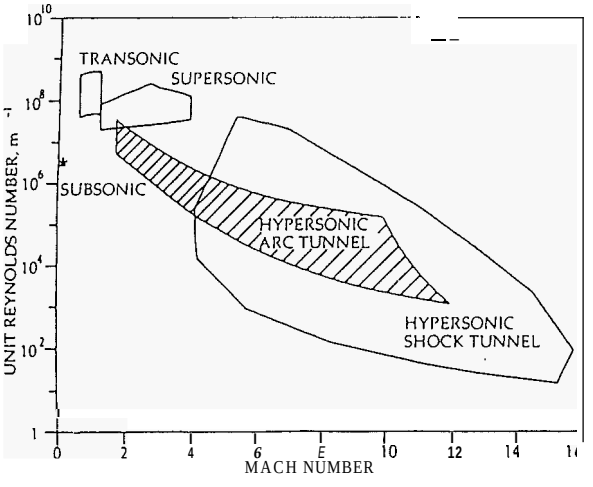

Fig. 1. Aerodynamics Research Center - Experimental simulation capability

A Thermal Dynamics Model F-5000 2.0 MW DC electric arc heater obtained from the Air Force Arnold Engineering Development Center (AEDC) provides the high-enthalpy gas flow for the facility. The arc heater was developed as part of the LORHO program[1-4] conducted at AEDC to investigate the feasibility of using MHD-augmented, electric arc heaters for hypersonic test facilities. Funding from the Permanent University Fund of the University of Texas System provided the support systems necessary to create an operational test facility.

A description of the facility together with initial performance data will be presented in this paper. Also, planned research programs using the arc heater to simulate the exhaust

---

Graduate Research Assistant, Dept. of Mechanical and Aerospace Engineering, Student Member
†Graduate Research Associate, Dept. of Mechanical and Aerospace Engineering, Student Member
Professor of Aerospace Engineering, Associate Fellow

conditions of a hydrogen-air supersonic combustor will be described.

Facility Description

An elevation view of the test facility configured for hypersonic aerodynamic testing is shown in Fig. *2,* and a schematic diagram showing the major components is presented in Fig. 3. These include the arc heater, nozzle, test section, diffuser and vacuum tank; and the supporting DC power supply, cooling water system, pneumatic system, vacuum system, and the facility instrumentation and data acquisition/-control system. Description of major flow-train components and facility support systems are provided in the following sections.

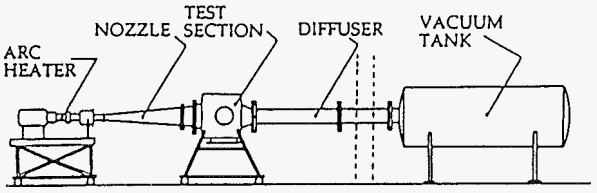

Fig. *2.* Elevation view - hypersonic arc tunnel

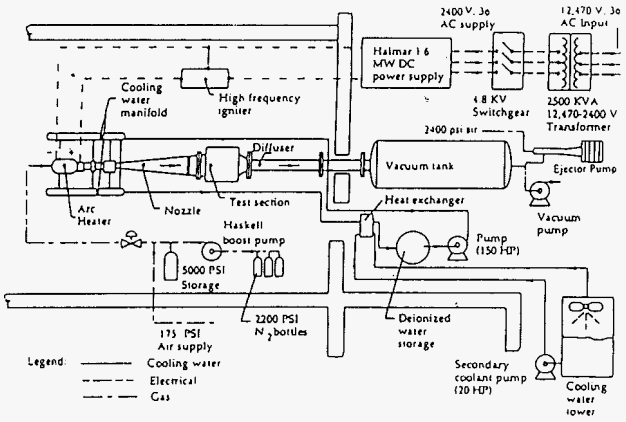

Fig. 3. Schematic diagram - hypersonic arc tunnel

Arc Heater

The Thermal Dynamics F-5000 arc heater is vortex-stabilized and nominally rated at *2.0* MW. A cross-sectional view of the heater is shown in Fig. 4. The anode, cathode, plenum chamber, and nozzle inserts are fabricated from beryllium-copper, and mounted in a brass housing that provides the necessary cooling water passages. The anode and cathode sections are electrically separated by a boron nitride insulator ring at the N_2 injection station. The anode section as well as the subsequent downstream components are grounded, whereas the cathode section is electrically floating. High pressure nitrogen gas is injected tangentially into the arc chamber through a swirl plate at the anode/cathode interface. This provides an intense vortex flow field within the arc chamber that centers the arc between a tungsten electrode at the base of the cathode barrel and the rotating arc termination point at the entrance to the plenum chamber downstream of the anode barrel. Provisions for injection of oxygen in the plenum chamber downstream of the arc termination point are provided to create "simulated air" for the subsequent nozzle expansion. These injection ports can also be used for injection of other gases to simulate the exhaust chemistry of hydrocarbon-air or hydrogen-air combustors for anticipated research programs involving hypersonic propulsion nozzle flow-field studies.

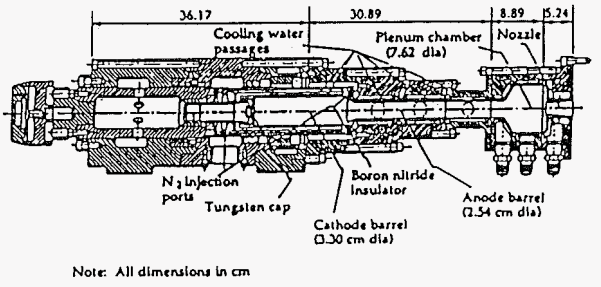

Fig. 4. Cross-sectional view, Thermal Dynamics F-5000 DC electric arc heater

The nominal open-circuit voltage is *2650* V. This is stepped-up by means of a high-frequency arc igniter circuit to initiate the electrical breakdown across a *0.76* mm gap between the anode and cathode barrels. The vortex motion induced by the tangential gas injection then stretches the arc to a nominal length on the order of 1 m. Maximum steady-state load voltage and current levels are *2000* V and *800* A, respectively, and are limited by the DC power supply.

Typical arc heater performance data from the original calibration at AEDC are shown in Fig. 5.

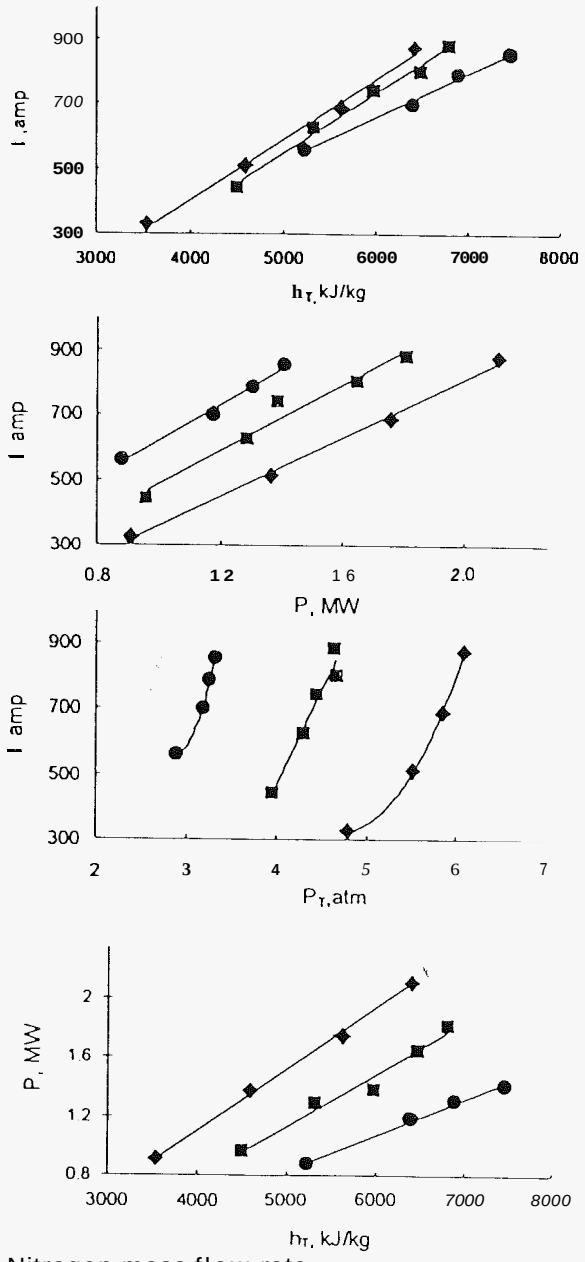

Fig. 5. Arc heater performance (from Ref. 2)

Nozzle. Test Section and Diffuser

A number of water-cooled nozzle inserts providing a range of Mach numbers from 1.8 to 4.0 were included with the arc heater when shipped from AEDC. A Mach 8 contoured nozzle developed as part of a hypersonic test facility at the LTV Aerospace and Defense Corporation[5] was also donated to UTA, but will require modification for cooling the nozzle throat for continuous operation.

The test section is a standard free-jet design. A maximum nozzle exit diameter of 20.3 cm (8 in) can be used, and the free-jet test section length from the nozzle exit to the diffuser entrance cone is 61 cm (24 in). The diameter of the test cabin is 76.2 cm. (30 in). Diagnostic probes or models can be inserted through a 25 cm (10 in) diameter port hole on the top of the test cabin or a 40.6 by 61 cm (16 x 24 in) model support plate in the bottom of the test cabin. Optical ports of 25.4 cm (10 in) diameter are located on each side of the test cabin to allow flowfield visualization via holographic interferometry or standard schlieren photography. A closed-jet test section, 20.3 cm (8 in) in diameter and 91.4 cm. (36 in) long is also available, if needed.

The diffuser has a 25.4 cm (10 in) capture diameter, and reduces to a 22.9 cm (9 in) constant throat diameter diffuser pipe that is 10.67 diameters in length. The diffuser ducts the flow out of the building and into a large vacuum tank. Design of the diffuser was adapted from the LTV hypersonic facility design[5].

Vacuum Tank

The vacuum tank is 107 cm (42 in) diameter, 345 cm (136 in) in length and has an internal volume of approximately 4.25 m^3 (150 ft^3). The criterion used to size the tank was the requirement to maintain established flow in the test section at the nominal arc heater flow rate, with auxiliary pumping of the tank by an air ejector pump. Initial evacuation of the tank is accomplished with a Sargent-Welch model 1396M vacuum pump.

Electrical System

A schematic drawing of the electrical system for the arc heater facility is shown in Fig. 6. The DC power supply is a Halmar 1.6 MW, current-regulated, plasma arc torch system, consisting of two Halmar model FRG-1 6-pulse current regulator and trigger circuits, a 12-SCR bridge rectifier, DC load-stabilizing choke,

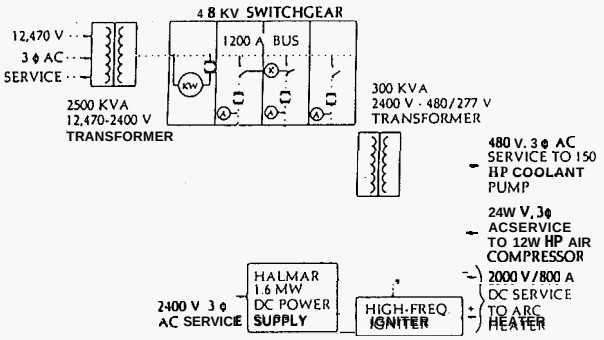

Fig. 6. Schematic diagram - electrical system

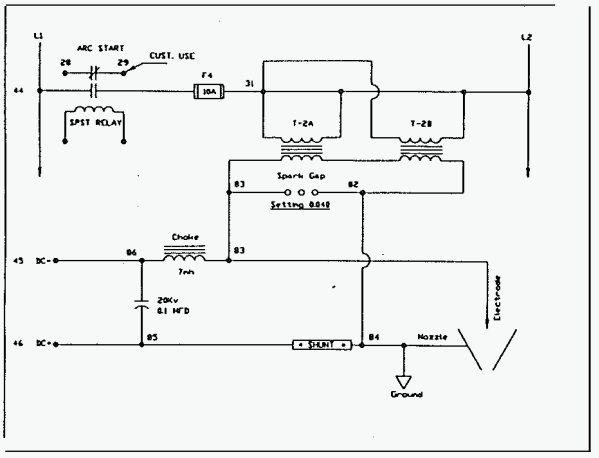

Fig. 7. Ignitor circuit

plasma torch interface unit, and associated control and alarm circuitry, interlocks, isolation transformer and interrupter switch. Three-phase AC power at 2400 V is supplied to the power supply from the ARC main transformer and switchgear panel. Maximum open circuit voltage of the DC power supply is 2650 V. The output from the power supply is fed to the terminals of the arc heater through a high-frequency igniter that provides the breakdown voltage necessary to initiate the arc. Maximum steady-state operating conditions are 2000 V/ 800 A. Current control regulation is ±1 percent of full scale current for a 10 percent line/load variation. The operating voltage, current, and power levels are both displayed on panel meters in the test facility control room for on-line monitoring, and transmitted to the facility data acquisition/control system.

The ignitor circuit (Fig. 7) produces a high voltage ripple (10 kV) which breaks down the gap between the cathode and anode, providing an ionized path for the power supply discharge to flow through. This ignition process produces severe electromagnetic interference (EMI). Thorough shielding was found to be necessary to prevent damage and limit interference with the control and data acquisition systems. The EMI from the ignitor box and the power cables going to the arc heater were contained by retrofitted shielding. However, the arc heater itself produced considerable EMI during ignition. This interference was strong enough to damage pressure transducers mounted in close proximity to the arc heater despite the shielding of the transducers. Accordingly, the replacement pressure transducers have been placed behind an aluminum panel, 2 m away from the arc heater, and are connected by nonconductive tubing. Care must also be taken to prevent the ignition voltage from feeding back into the DC power supply causing damage. An undetected short in the choke coil of the ignitor circuit resulted in the destruction of the power supply control circuit by high voltage during initial checkout of the system. Additionally, the original 0.001 mF capacitor in the LC filter of the ignition circuit had to be replaced with a 0.1 mF capacitor to bring the feedback down to tolerable levels.

High-Pressure, Deionized Coolina Water Svstem

A schematic of the high-pressure, deionized cooling water system is shown in Fig. 8. The system consists of a Water Systems, Inc. 1500 ℓpm (400 gpm)/ 2340 kPa (340 psi) pump station, a high-pressure, closed-loop, deionized piping system connected to the test facility; and a low pressure piping system used to reject heat to cooling tower of the ARC compressor plant. The high-pressure deionized cooling water is piped to and from the supply and discharge manifolds, where separate, parallel cooling water lines are connected to the anode, cathode, plenum chamber, nozzle, test section/diffuser, and DC power supply. The flow rate, temperature rise and pressure drop for each line are monitored on panel meters in the control room, and critical measurements are fed directly into the facility data acquisition/-control system. A separate cooling water line is also available for cooling diagnostic probes or models inserted into the flow stream.

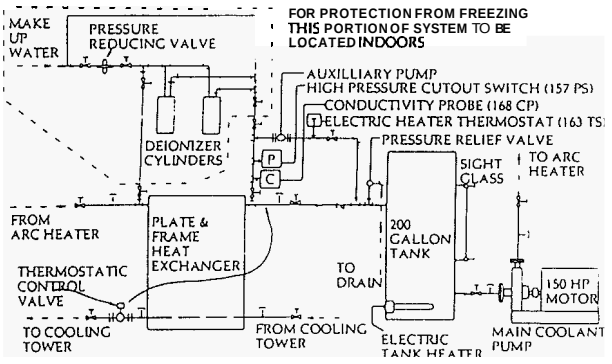

Fig. 8. Schematic diagram - Deionized cooling water system.

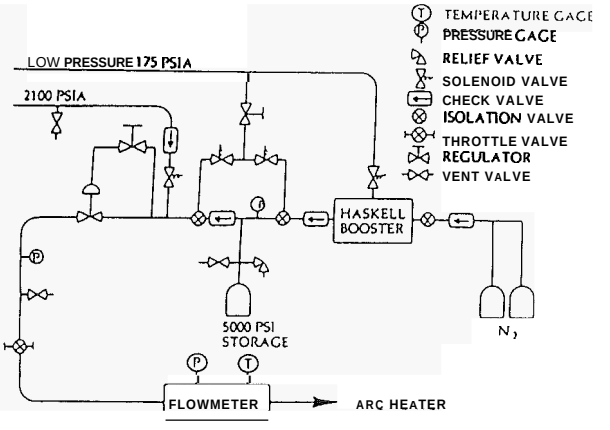

Fig. 9. Schematic diagram - pneumatic system

Pneumatic System

A schematic drawing of the pneumatic system is shown in Fig. 9. The high-pressure nitrogen system consists of standard 15 MPa (2200 psi) N_2 bottles manifolded together and connected to a Haskel model 29498 two-stage, gas-driven booster pump. The output from the Haskel pump is used to pressurize a 34.5 MPa (5000 psia) storage bottle that is used to drive the arc heater in a blow-down mode. The system is currently sized to provide 1 minute of operation at a nominal flow rate of 0.15 kg/sec (0.33 lbm/sec). Recharge time to refill the storage bottle is approximately 20 minutes. The discharge from the storage bottle is regulated by a TESCOM model 26-1221 regulator, and the flow rate is monitored by a Flow-Dyne critical flow nozzle. Low pressure 1200 kPa (175 psi) control air for operation of the Haskel boost pump, and for remote activation of the control valves during operation of the arc heater is provided by the ARC low-pressure air supply network. Provisions for supplying 16.5 MPa (2400 psi) air from the ARC high-pressure compressor plant[6] are also available, and will be used for a variety of cold-flow and mixed-flow tests that are anticipated.

Vacuum System

A Sargent-Welch model 1396M vacuum pump rated at 2.0 μm and 2800 ℓpm (100 cfm) is used for initial evacuation of the vacuum tank. An air ejector pump is being developed to sustain the vacuum during a test run. The ejector pump was designed by a team of students, and is currently being fabricated. A primary flow of compressed air of up to 4.0 kg/s will entrain a secondary flow from the arc heater of up to 0.4 kg/s. The 750 kg storage capacity of the compressed air storage bottles[6] will permit several arc heater firings before having to recharge these bottles. The ejector pump will discharge into a silencer to minimize the acoustical noise. A vacuum tank pressure of 13.8 kPa (2.0 psia) was chosen as the design point for the ejector pump. It is anticipated that the test section can be maintained at a lower pressure than the vacuum tank due to the formation of an oblique shock train in the connecting diffuser sections.

Instrumentation System

The facility instrumentation system provides measurements of parameters needed for facility set-up and on-line operational monitoring during testing, as well as parallel measurements of critical parameters needed for determination of the facility operational performance. These measurements include the arc heater voltage, current and power; inlet gas flow rate, pressure and temperature; cooling water flow rate, pressure drop and temperature rise; arc heater plenum chamber total pressure, nozzle static pressure distribution, and test section static and total pressure.

These measurements are read into a data reduction program to determine the following critical facility performance parameters; total enthalpy level, plenum chamber and test section total pressure, nozzle and test section static pressure. The total enthalpy level is

determined by standard energy balance procedures,

$$h_T = \frac{1}{\dot{m}_g}\left[\left(\dot{m}C_pT_i\right)_g + IV - \Sigma\left(\dot{m}C_p(T_o - T_i)\right)_{cw}\right]$$

where h_T = gas total enthalpy
$\dot{m}_g$ = gas mass flow rate
T_i = inlet temp
C_p = constant pressure specific heat
I = current
V = voltage
T_o = outlet temp
cw = cooling water

Total pressure and enthalpy profiles will be measured using a water-cooled total pressure and enthalpy probe design which was developed at AEDC[3]. A precision three-axis probe traverse system has been designed to perform probe surveys of the flow. The system is driven by a single stepper motor which is multiplexed to three axes by toothed belts running to electromagnetic clutch-brakes corresponding to each axis. Motion routines are pre-programmed prior to a test run. During the run, the data acquisition system provides triggers to cue the stepper motor driver to initiate the next movement. The primary sources of positional error are expected to be thermal expansion and vibration of the traverse mechanism. Apart from these effects the mechanism is design to be accurate within ±0.64 mm.

Data Acquisition/Control System

The data acquisition system for the test facility consists of a Hewlett-Packard model 3852A Data Acquisition/Control System, interfaced via an IEEE 488 interface bus to a HP Vectra model 45 host computer. A schematic of the system is shown in Fig. 10. Twenty channels of low-speed data acquisition (12 Bit/5.5 kHz) are available for facility monitoring, and twenty-four channels of moderate-speed data acquisition (12 Bit/100 kHz) are provided for model instrumentation. In addition, the data acquisition systems for the impulse facilities in the adjoining High-speed Aerodynamics Lab[6] are available for special tests requiring high data rates. These include a 48-channel, 100 kHz/channel DSP Technology System, an 8-channel, 5 MHz LeCroy System, and a 2-channel, 300 MHz Hewlett-Packard digital storage oscilloscope.

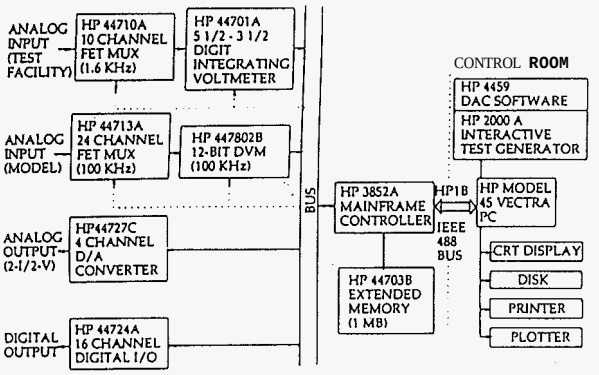

Fig. 10. Schematic diagram - data acquisition system

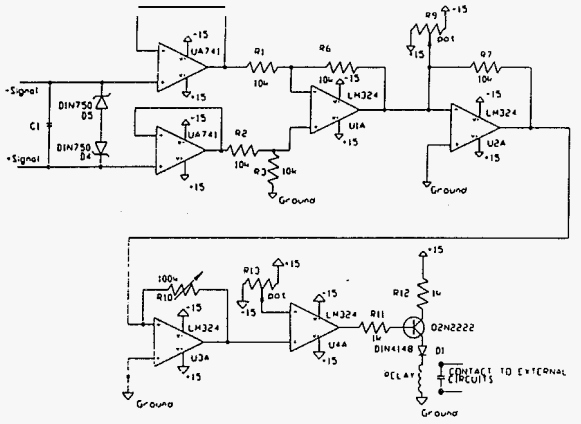

Fig. 11. Analog comparator circuit

Past operations at AEDC have emphasized the need to rapidly shut off the electricity to the arc heater, in the event of an interruption of gas or cooling water flow, to prevent major damage. The data acquisition system was originally intended to fulfill this function, but was found to respond too slowly. A vastly superior reaction time has been obtained through the adoption of analog comparator circuits (Fig. 11). Each critical process is continuously monitored by a dedicated circuit which shuts off the arc heater power supply when a measured parameter crosses a threshold value. The reaction time, which is primarily limited by

the operating time of the relays involved, is estimated to be less than 30 ms.

Facilitv Performance Estimate

The estimated operational performance capability of the test facility was shown in Fig. 1. This estimate was based on the prior arc heater performance data from the AEDC calibration (Fig. 5), with corrections for the anticipated plenum chamber pressure increase associated with the intended operation of the arc heater with smaller nozzle throat diameters than used in the original calibration. The nozzle expansion calculations were done with the NASA CEC76 nozzle flow code[7], with boundary layer corrections from a nozzle boundary layer code developed at JPL[8]. The variation in Mach number shown in Fig. 1 will be achieved by using a range of small nozzles (low end) or a single nozzle with interchangeable throat inserts (high end).

Initial Operational Results

Data Reduction

A plot of cooling water temperature vs. time for a typical run is shown in Fig. 12. The output from the thermocouples was troublesome due to the large scale noise on the signals. This problem is primarily due to the output from the type T thermocouples typically being less than 10 mV. Accordingly, subsequent processing of these data is necessary to reduce the scatter in the gas total enthalpy results derived from the energy balance calculations. The first step is identifying the window of data during the run where the temperatures are steady. Next, any points outside approximately 2.5 standard deviations (Chauvenet's criteria) for a test window are discarded and replaced with the mean temperature for the window. Finally, a least squares linear curve fit is applied to these data which gives the values to determine the temperature differences for the energy balance (Fig. 13). In the future, this difficulty will be circumvented by using RTD's, with much higher outputs than thermocouples. The uncertainty in the final data could have been further reduced by increasing the cooling water ΔT's across the

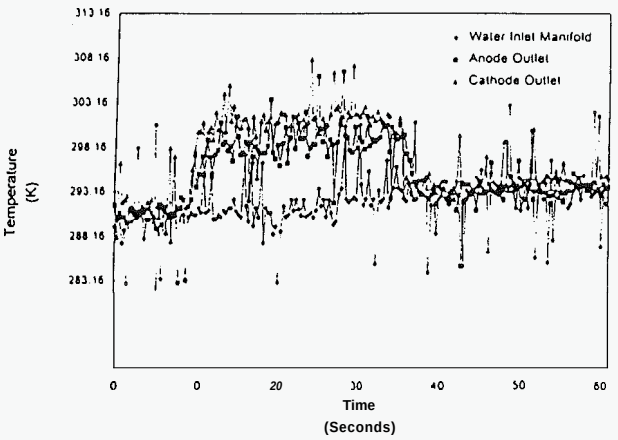

Fig. 12. Typical cooling water temperature-time traces

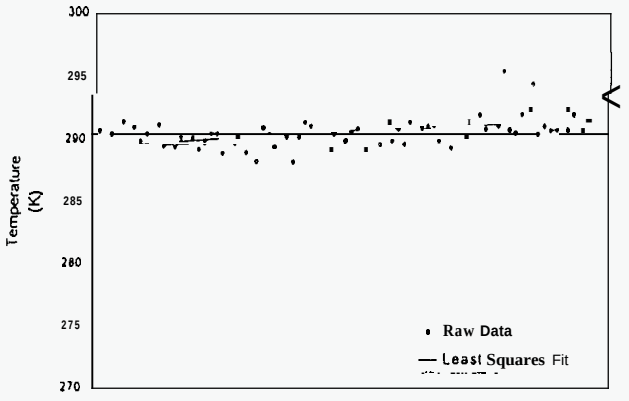

Fig. 13. Least squares curve fit of temperature data

arc heater. However, it was not known, from the history of this arc heater's operation at AEDC, what risk of failure the lower cooling water flow rates posed.

The raw data of the current and voltage measurements also show fluctuations (Fig. 14), but this is not believed to be noise because the power signal, which comes through the same cable, is smooth. The dynamics of the vortex stabilized arc does create voltage fluctuations for which the power supply has to compensate to maintain a stable current. Accordingly, the average current is constant, although there are instantaneous fluctuations. Linear least square curve fits were applied to the voltage and current data to reduce them for the total enthalpy calculations.

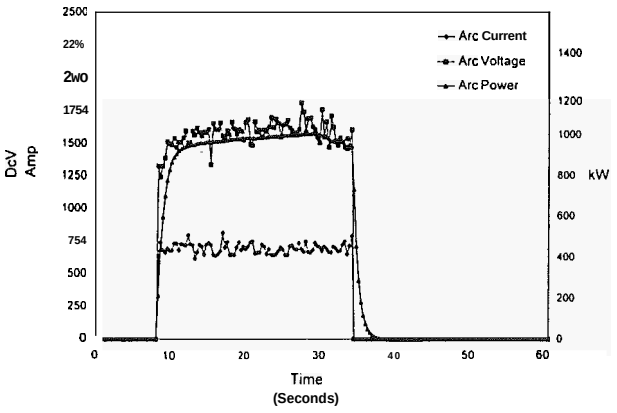

Fig. 14. Arc heater power, current and voltage vs. time

Due to an unforeseen flow constriction at the outlet of the gas storage tank, a steady gas mass flow could not be maintained over a long enough period to acquire data for rates higher than 0.1 kg/s (Fig. 15 and Fig. **16).** Once this problem is corrected, steady operation at rates of 0.3 kg/s or more should be attainable. The gas mass flow constraint has a secondary effect in limiting the voltages that can be obtained to less than the 2000 V maximum the power supply is capable of. This peak voltage was reached during some of the unsteady runs. Limitations were also encountered with the current to which the arc heater could be set to operate. At current settings at or below 450 A, instability was observed in the plume. It is expected that higher gas mass flow rates should allow stable operation at lower current settings. At high current settings approaching 700 A, instantaneous current fluctuations caused the power supply to shut down due to an overcurrent trip. This problem may be remedied to some degree by adjusting the trip level upward on the power supply control circuit, which must be done in consultation with the manufacturer.

Arc Heater Performance Mar,

The results from the initial operation of this facility reveal similar trends to the operation of the arc heater at AEDC. Unfortunately, the new data are confined to a narrower range of gas mass flow rates than the AEDC data. However, this is not a permanent constraint; operation at higher gas flow rates will be possible in the near future. Additionally, this

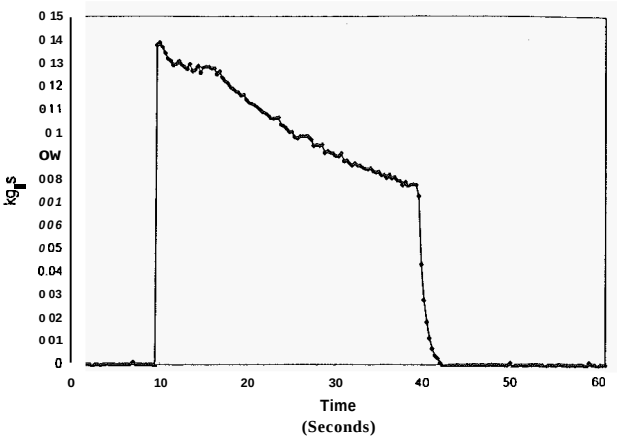

Fig. 15. Nitrogen mass flow rate - constriction limited

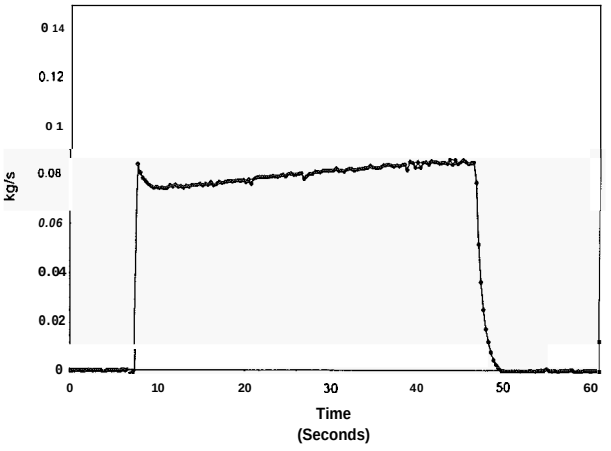

Fig. 16. Nitrogen mass flow rate with unrestricted regulator

new data was obtained with a different nozzle than the original nozzle used for the AEDC data presented, since the original nozzle needs to be refurbished. The bulk total enthalpy is observed to increase almost linearly with both increasing current and power (Fig. 17 and Fig. 18). This indicates that arc heater efficiency varies only slightly over the range of operation presented. Also decreasing the gas mass flow causes the bulk total enthalpy to rise, due to there being less gas to absorb the input electrical energy. Plenum pressure shows a weak dependence on input current, consistent with the AEDC data (Fig. **19).** The primary means of manipulating plenum pressure will be using nozzles with differing throat areas. Accordingly, a much broader range of operation is obtainable with this facility than the range presented from this initial operation.

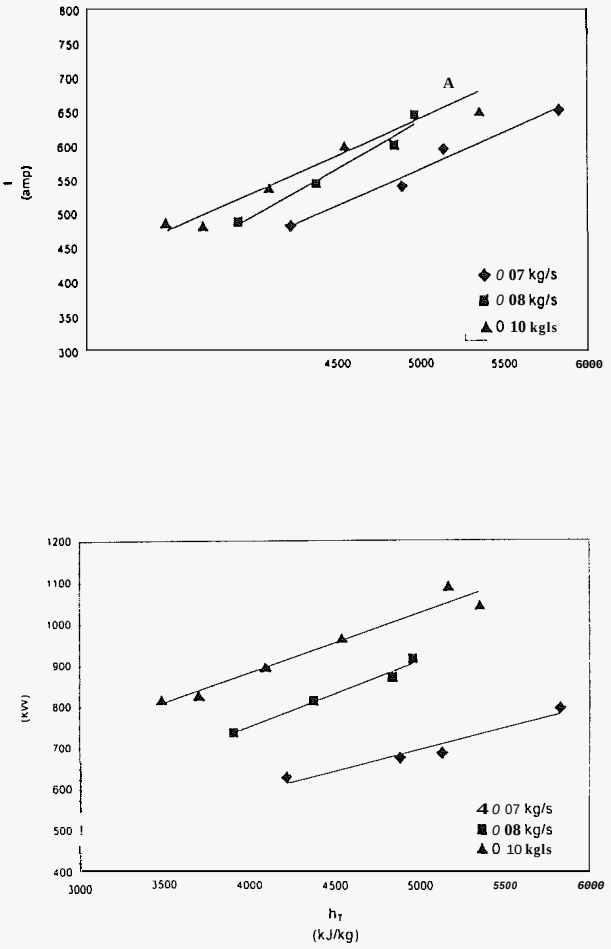

Fig. 18. Arc power vs. total enthalpy

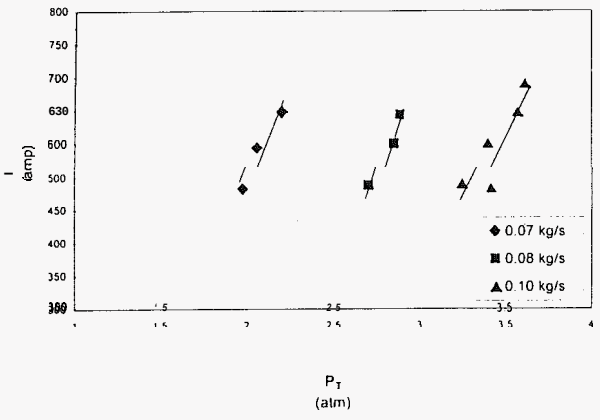

Fig. 19. Arc heater total pressures

Hypersonic Propulsion Nozzle Simulation

An area of promising research made possible by the development of the arc-heater facility is the investigation of flow phenomena associated with hypersonic propulsion nozzles, with particular emphasis on nozzle/airframe flow field interactions for off-design operation of the nozzle. The operational characteristics of the arc heater are such that a reasonable simulation (Mach number, pressure and temperature) of the exhaust from supersonic combustors is possible. Furthermore, by injecting a proper mixture of secondary gases into the arc heater plenum chamber, a realistic simulation of the chemistry of the combustor exhaust products is also possible[9,10].

Fig. 20 shows a sketch of the modified plenum chamber. Controlled amounts of hydrogen and oxygen gas will be injected into the plenum chamber to mix with the hot nitrogen plasma exiting from the anode barrel. Preliminary calculations indicate that the gasdynamic conditions (pressure, temperature and Mach number) and chemical composition of a representative hydrogen-air supersonic combustor can be closely matched up to flight Mach numbers of 6-7[11]. Beyond this range, the chemical reactions occurring at the low plenum chamber Mach numbers require excessive heating of the nitrogen to simulate the combustor exhaust enthalpy.

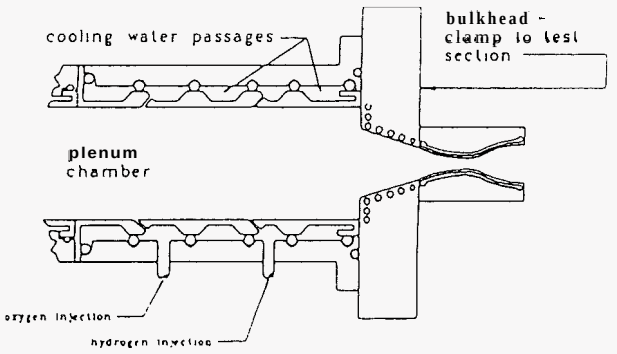

Fig. 20. Modified plenum chamber

The nitrogen-hydrogen-oxygen mixture will be expanded through a rectangular (3:1 aspect ratio) nozzle to representative combustor exhaust Mach numbers of 1.5 to 2.0. A single expansion ramp nozzle has been designed to investigate the effects of chemical and thermal nonequilibriun on nozzle performance (Fig. 21). Data will consist of surface pressure and heat transfer rate measurements, total pressure and enthalpy probe surveys, and schlieren flow field visualization. The data from the simulated hydrogen-air combustor will be compared with

data from tests to be conducted with a cold-flow argon-freon test gas. An argon-freon mixture is commonly used in nozzle tests due to its ability to simulate the correct specific heat ratio of a hydrogen-air combustion gas[12]. Although this technique has been used with success in experimental investigations of blunt body flows, there is some question as to its validity for expanding flows with large-scale changes in chemical composition[13].

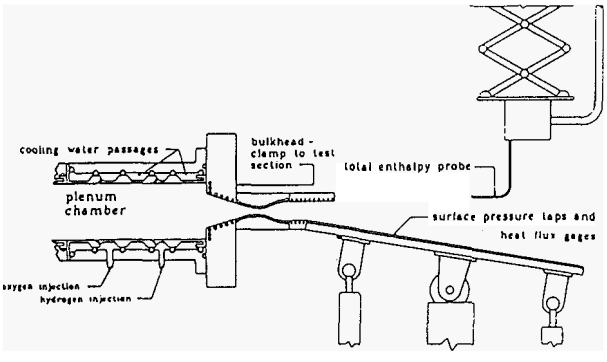

Fig. 21. SERN model

The test section pressure will initially be set to simulate design point operation of the nozzle, and the major objective of the investigation will be the determination of the importance of correct simulation of the chemical composition on nozzle performance measurements. Subsequent studies will explore the influence of nonequilibrium flow phenomena on off-design performance of the nozzle. Initial simulation of off-design operation will utilize a "wind-off" approach, in which the exhaust tank pressure will be set at pressure levels representative of both under-expanded and over-expanded nozzle operation. Ultimately, we hope to add an external hypersonic flow simulation *so* that the effect of shear layer mixing on off-design operation can also be simulated. Flow-field interactions resulting from off-design nozzle operation have been examined by CFD simulations[4-17], but little experimental data appears to be available to validate these calculations with correct experimental simulation of the combustion gas chemistry.

Concludina Remarks

A continuous-flow, arc-heated, hypersonic test facility has been put into operation at UTA, and its performance map is currently being determined. Initial calibration data suggest that the basic arc heater performance demonstrated in development tests conducted at AEDC can be replicated. The current-controlled power supply provides a stable mode of operation that is easily controlled. During the initial operation, the enthalpy levels required for future propulsion simulation experiments were achieved. Minor facility modifications should increase the operational envelope well beyond that obtained from the initial operation.

In summary, the arc-heated hypersonic test facility should not only provide a valuable complement to the aerodynamic testing capability of the existing hypersonic shock tunnel at UTA, but in addition should provide a unique test capability for investigation of a variety of phenomena that cannot easily be done in short-duration test facilities. In particular, the new facility appears to offer a unique capability for investigation of the effect of chemical and thermal nonequilibrium on the performance of hypersonic propulsion nozzles.

Acknowledaments

This effort is part of the research program of the NASA/UTA Center for Hypersonic Research, supported by NASA Office of Aeronautics under NASA Grants NAGW-3714 and NAG 1 1798. The NASA project monitor is Dr. Isaiah Blankson. The UTA Center is also supported by Lockheed Martin Tactical Aircraft Systems (formerly Lockheed Fort Worth Company) through grant #4286428, monitored by Dr. J. V. Clifton.

References

1. Browning, J.A. and Poole, J.W., "Arc Gas Heaters-Present and Future," paper presented at AGARD Specialists' Meeting on Arc Heaters and MHD Accelerators for Aerodynamic Purposes, Rhode-Saint-Genese, Belgium, September 21-23, 1964.

2. Tempelmeyer, K.E., Windmueller, A.K., and Rittenhouse, L.E., "Development of a Steady-Flow JxB Accelerator for Wind Tunnel Application," paper presented at AGARD Specialists' Meeting on Arc

Heaters and MHD Accelerators for Aerodynamic Purposes, Rhode-Saint-Genese, Belgium, September 21-23, 1964.

3. Wilson, D.R. and Rittenhouse, L.E., "Experimental and Theoretical Gasdynamic and Electrical Performance of a 400 kW MHD Accelerator," *Proceedings of the 5th Hypervelocity Techniques Symposium*, Denver, Colorado, May 16-17, 1967.

4. Rittenhouse, L.E., Whoric, J.M., and Wilson, D.R., "Experimental and Theroretical Results Obtained with a Linear MHD Accelerator Operated in the Hall Current Neutralized Mode," AEDC TDR 67-150, November 1967.

5. Stalmach, C.J., Jr., "Design and Operation of a Variable-Volume Arc Chamber in a Hypervelocity Wind Tunnel," *Proceedings of the 4th Hypervelocity Techniques Symposium,* Arnold Engineering Development Center, Tennessee, 1965.

6. Wilson, D.R., "Development of The University of Texas at Arlington Aerodynamics Research Center," AIAA 88-2002, *Proceedings of the AIAA 15th Aerodynamics Testing Conference,* San Diego, California, May 18-20, 1988.

7. Gordon, S. and McBride, B. J., "Computer Program for Calculation of Complex Chemical Equilibrium Compositions, Rocket Performance, Incident and Reflected Shocks, and Chapman-Jouguet Detonations," NASA SP-273, 1971.

8. Elliot, D.G., Bartz, D.R. and Silver, S., "Calculation of Turbulent Boundary-Layer Growth and Heat Transfer in Axi-symmetric Nozzles," JPL TR 32-387, February 1963.

9. Agnone, A.M., "NASP Exhaust Plume Simulation with the Ames 16" Shock Tube," AIAA 88-2054, *Proceedings of the AIAA 15th Aerodynamic Testing Conference,* San Diego, California, May 18-20, 1988.

10. Kim, B., Stoy, S. and Fivel, H., "Arc Heater Nozzle Heating Test with Hydrogen Combustion Products," AIAA Paper 91-1413, AIAA 26th Thermophysics Conference, Honolulu, Hawaii, June 24-26, 1991.

11. Bhatt, J., "Simulation of Combustion Chemistry of a Scramjet," M.S. Thesis, The University of Texas at Arlington, August, 1996.

12. Hopkins, H.B., Konopka, W. and Leng, J., "Validation of Scramjet Exhaust Simulation Technique at Mach 6," NASA CR 3003, March, 1979.

13. Wagner, D.A., Smith, R.K., Gunn, J.A. and Hasegawa, S., "Hypersonic Test Facility Requirements for the 1990's," AIAA Paper 90-1389, AIAA 16th Aerodynamic Ground Testing Conference, Seattle, Washington, June 18-20, 1990.

14. Harloff, G.J., Lai, H.T., and Nelson, E.S., "Two-Dimensional Viscous Flow Computations of Hypersonic Scramjet Nozzle Flowfields at Design and Off/Design Conditions," AIAA Paper 88-3280, 1988.

15. Harloff, G.J., Reddy, D.R., and Lai, H.T., "Viscous Three-Dimensional Analysis of Nozzles for Hypersonic Propulsion," NASA Contractor Report 185197, January, 1980.

16. Huebner, L.D. and Tatum, K.E., "Computational and Experimental Aftbody Flow Fields for Hypersonic, Airbreathing Configurations with Scramjet Exhaust Flow Simulation," AIAA Paper 91-1709, AIAA 22nd Fluid Dynamics, Plasma Dynamics & Lasers Conference, Honolulu, Hawaii, June 24-26, 1991.

17. Huebner, L.D. and Tatum, K.E., "CFD Code Calibration and Inlet-Fairing Effects on a 3D Hypersonic Powered-Simulation Model," AIAA Paper 93-3041, AIAA 24th Fluid Dynamics Conference, Orlando, Florida, July 6-9, 1993.